# Experimental Analysis of High Reynolds Number Aero-Structural Dynamics in ETW

J. Ballmann[*]

*RWTH Aachen University, Aachen, 52062, Germany*

A. Dafnis[†], H. Korsch[†], C. Buxel[†], H.-G. Reimerdes[†],
K.-H. Brakhage[‡], H. Olivier[§]
C. Braun[*], A. Baars[*], A. Boucke[*]

**The paper reports about the aero-structural dynamical experiments with an elastic wing model which were conducted during the High Reynolds Number Aero-Structural Dynamics project by RWTH Aachen University in the cryogenic European Transonic Windtunnel, with funding from the German Research Foundation. The static and dynamic experiments have been performed in transonic flow at different windtunnel conditions concerning Reynolds number (up to 73 millions) and dynamic pressure (up to $0.13MPa$). Starting with the description of the wing model, the measuring equipment and envelopes of the experiments, selected results of static and dynamic experiments are presented, partly in comparison with results obtained from numerical predictions during the preparation phase of the specimen and the experiments. For this the Computational Aero-Structural Dynamics package SOFIA of RWTH Aachen University was used. Results have been collected in a data base which will be made freely accessible to the aerodynamic and aeroelastic community in the near future.**

## I.   Introduction

Transonic aeroelastic windtunnel testing with scaled wing models uses to be conducted hitherto in windtunnels at Reynolds numbers which are about one order of magnitude less than in real cruise flight of large passenger aircrafts [1]. Only very few aeroelastic windtunnel experiments with oscillating elastic wings have been performed, so far, in the transonic flow regime at flight Reynolds numbers of large transport aircrafts. For an airfoil in transonic flow with prescribed oscillation buffet has been examined at high Reynolds number in a cryogenic environment at NASA LaRC [2].

Besides the necessity for a thorough understanding of aeroelastic phenomena windtunnel experiments with elastic wings at high Reynolds numbers are necessary for validating methods of multidisciplinary airplane design and for realistic Computational Aero-Structural Dynamics (CASD) simulation of airplanes in flight. Normally data form aeroelastic experiments is declared confidential and not open for university research. Thus the objectives of the High Reynolds Number Aero-Structural Dynamics (HIRENASD) project, which was funded by the German Research Foundation (DFG) through the Collaborative Research Centre "Flow Modulation and Fluid-Structure Interaction at Airplane Wings" (SFB 401), are twofold. First, of course, to gain better aero-structural dynamics understanding and knowledge in the transonic regime up to real flight Reynolds numbers and, second, to obtain experimental data in a wide range of Reynolds numbers and aerodynamic loads for current and future aerodynamic and aeroelastic research.

So-called Collaborative Research Centres like SFB 401 which are funded by DFG in Germany represent volontary associations of different university chairs for long term multidisciplinary research up to 4 subsequent research periods of 3 years each. In case of SFB 401 Chairs of Mathematics, Mechanics and Computational

---

[*]Department of Mechanics (LFM), Templergraben 64, 52062 Aachen, Affiliate AIAA member.

[†]Institute of Leight Weight Structures (ILB), Wüllnerstrasse 7, 52062 Aachen

[‡]Institute of Geometry and Practical Mathematics (IGPM), Templergraben 55, 52062 Aachen

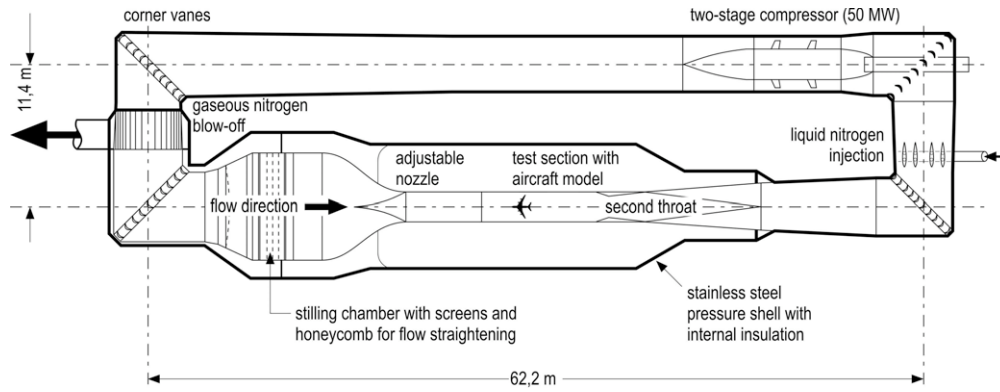[§]Shock Wave Laboratory (SWL), Schurzelterstraße 35, 52074 Aachen

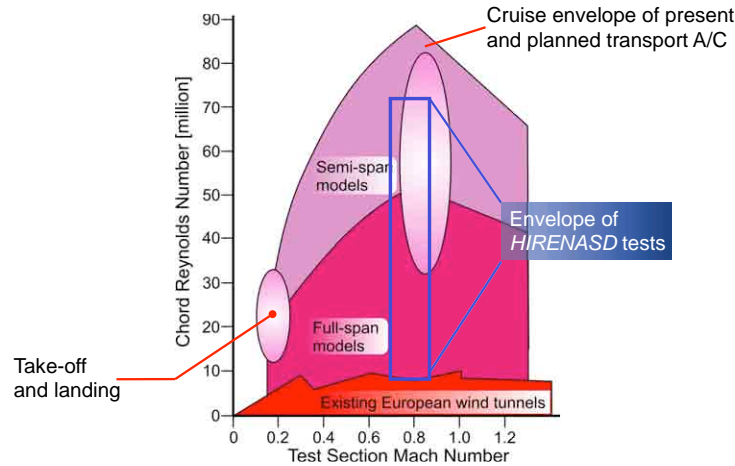**Figure 1. The European Transonic Windtunnel circuit.**



**Figure 2. Test envelope of the European Transonic Windtunnel in comparison with other European windtunnels.**

Analysis of Technical Systems, Aerodynamics, Shock Waves, Aeronautics and Astronautics, Flight Dynamics and Light Weight Structures are cooperating. The very expensive experimental project HIRENASD is a special central project which has been initiated after 7 years of successful research work of SFB 401. An overview of this work is presented in [3]. The HIRENASD project has been conducted in strong cooperation of the four member chairs LFM, ILB, IGPM and SWL of the centre and included the layout of the model and the experiments, the design of the model and vibration excitation mechanism, the design and construction of a new windtunnel balance, the manufacturing of all this and equipment with 5 different measuring techniques.

The wing model corresponds to the SFB 401 clean wing reference configuration [4], which has a planform as typical for large passenger transport aircrafts, with $34^o$ sweep angle and the supercritical wing profile BAC 3-11 reported in AGARD-AR-303 [5], which has been arranged for cruise flight [3]. The complete windtunnel assembly has a span of $1.375m$ . The aerodynamic mean chord of the wing model is $c_{ref} = 0.3445m$. The windtunnel experiments in ETW include static and dynamic aeroelastic measurements at different windtunnel flow conditions, in total 51 conditions for steady polars and 135 conditions for dynamic tests. First, without vibration excitation, the pressure distribution, lift and drag polars were measured from negative angles ($\alpha = -2^o$) to positive angles (maximum $\alpha = +5^o$) of incidence. After evaluation for the zero lift angle of incidence, excited vibration tests were performed at this angle. Chosen Mach numbers were Ma = 0.7, 0.75, 0.8, 0.83, 0.85 and 0.88. The mentioned windtunnel conditions were at mainly 3 different values of q/E $= 0.22 \cdot 10^{-6}, 0.34 \cdot 10^{-6}$ and $0.48 \cdot 10^{-6}$ which is the ratio of dynamic pressure and Youngs Modulus of the wing model, and for different Reynolds numbers up to 73 millions in one series of experiments with q/E $= 0.7 \cdot 10^{-6}$. Vibrations were excited in the dynamic experiments at three different frequencies near resonance. The paper is organised as follows: In section II the windtunnel is shortly described, section III presents
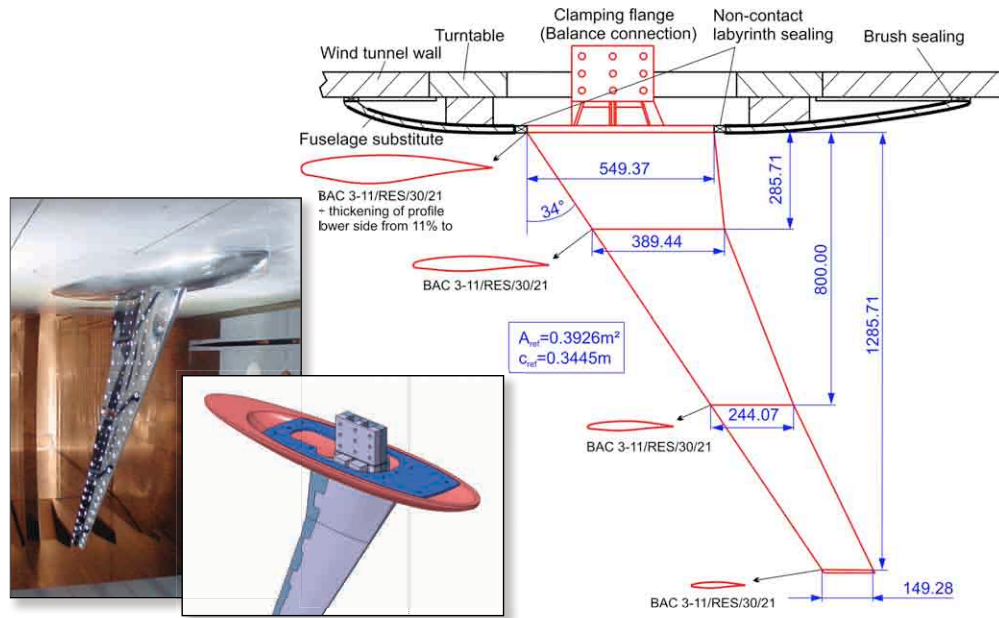
American Institute of Aeronautics and Astronautics

**Figure 3.  Windtunnel model dimensions and its placement in the windtunnel (photograph).**

a description of the windtunnel model and its instrumentation and in section IV static and dynamic test results will be presented.

## II.    The European Transonic Windtunnel (ETW)

The European Transonic Windtunnel is a cryogenic facility with closed circuit, see figure 1. The fluid is nitrogen gas. Flow conditions can be chosen as follows: fluid temperatures from $110K$ to $313K$ and the total pressure from $0.125MPa$ to $0.45MPa$. The dimensions of the test section are height $2.0m$, width $2.4m$ and length $9.0m$. The nozzle is adjustable, walls in the measuring section can be chosen slotted or closed and a second throat is present behind the test-section. Controlled liquid nitrogen injection and gaseous nitrogen blow-off maintain temperature and pressure at the chosen level and a two-stage $50MW$ compressor provides Mach numbers from Ma = 0.15 to Ma = 1.3. Mach number can be very quickly adjusted to a chosen value. This opportunity was indeed needed because of the enormous data flow that required a certain time for data storage after each of the 186 experiments. During these pauses the Mach number was reduced to save liquid nitrogen and energy.

Under the lowest temperature condition and static pressure around $0.4MPa$, it is possible in ETW to achieve Reynolds numbers of up to 80 millions in half-model testing at transonic Mach numbers [6], with the aerodynamic mean chord as reference length, see figure 2. Special model material is needed for the elastic wing model to procure its toughness and elasticity under high aerodynamic loads at temperatures from $110K$ to $310K$ [7]. One advantage of ETW is that the parameters Mach number, Reynolds number and dynamic pressure, or even more adequate, the ratio of dynamic pressure to Youngs modulus of the model material, which are influencing the aeroelastic behaviour of the wing [8, 9, 10], can be varied independently of each other.

## III.    Windtunnel Model Assembly and Measuring Equipment

### III.A.    Windtunnel Model Assembly

The planform of the elastic wing model has the typical characteristics of a wing for a large passenger aircraft as mentioned in the introduction. The leading edge sweep angle is $34^o$, the span of the wing model from root to tip is $1285.71mm$, and the chord decreases from its root value over three sections piecewise linearly to the tip value. The wing model is untwisted such that the leading edge and the twice kinked trailing edge
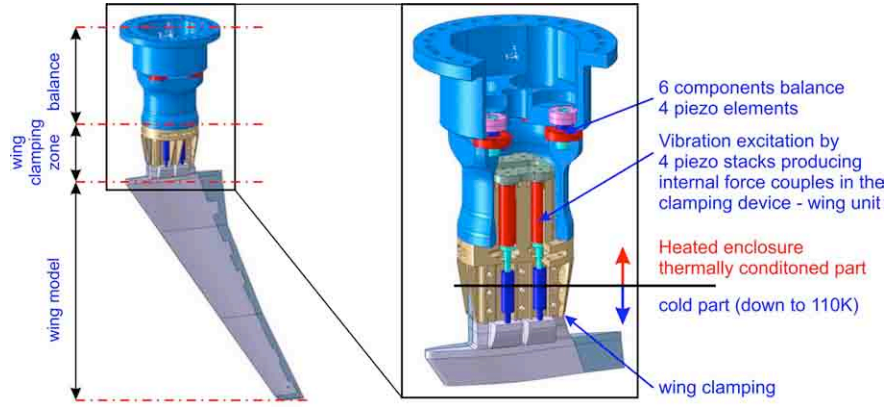
American Institute of Aeronautics and Astronautics

**Figure 4. Windtunnel balance and vibration excitation mechanism.**

are positioned in a common plane. Figure 3 contains the chord length values at the wing root and tip and at the two kinks. The values at root and tip are $549.31mm$ and $149.29mm$, respectively. The aerodynamic mean chord and planview wing area are $c_{ref} = 0.3445m$ and $A_{ref} = 0.39255m^2$. The profile in the two outer sections is the BAC 3-11 profile which has 11% thickness and was taken from [5]. In the wing root section the upper wing side has this profile too, only the bottom surface of this section has been linearly thickened to a total profile thickness of 15% at the wing root.

The model consists of two pieces, the upper and the lower part which have a jointing surface with straight separation line along the leading ledge and a meandering separation line on the bottom surface of the model, as can be seen on the bottom side view of the wing model in figure 5. To impede relative motion of the model parts, a grooved and tongued joint concept with form-locking has been applied in span- and cross-direction along the jointing surface. This can be seen in figure 5, which shows the interior of the top and bottom parts of the wing model, where one can recognise seven ribs for implementation of pressure sensors and three stringers in longitudinal direction, of which the central ends at about 60% span. Because of the large range of temperature from $110K$ to $310K$ and the high dynamic pressure up to $0.13MPa$ a highly tenacious material was selected for the elastic model which almost maintains its properties over the full range of dynamic pressure and temperature according to the envelopes of the experiments. The material of choice was a C200 Maraging steel (G90c) with $18^0$ Nickel [7].

In order to alleviate the influence of the ceiling boundary layer of the windtunnel, where the model was mounted on a plate fixed at the turntable as for half-model testing, a fuselage substitute is provided around the wing as shown in figure 3. It has no mechanical contact with the elastic wing model. A round arch labyrinth sealing is implemented on the fuselage substitute side which surrounds the wing root. Thus the complete wetted surface in the windtunnel looks much like a wing body half-configuration with a total span of $1375mm$.

The total windtunnel model assembly consists of the wing model, the wing clamping, a new, very stiff windtunnel balance which is fixed with its base in the heated enclosure which is attached outside at the windtunnel wall, as shown in figure 6.

Forced vibration of the windtunnel model is realised by dynamic force couples made up by four spanwise directed forces which are applied at prominent noses of the wing root. These can be seen in figure 4. The whole mechanism is integrated in a housing which is part of the wing clamping such that the forces generated by four pre-stressed piezo-stacks act as interiour force couples between the bottom of the housing and the prominent noses at the wing root, whereby the force transmitting struts are made from the same material as the wing model, as well as the excitation mechanism housing, for thermal extension reasons.

### III.B.  Measuring Equipment

*III.B.1.  Force Measurement*

As already mentioned a new 6-components windtunnel balance based on four piezo-electric load cells has been designed and built for force measurement in the dynamical aeroelastic experiments because the installed
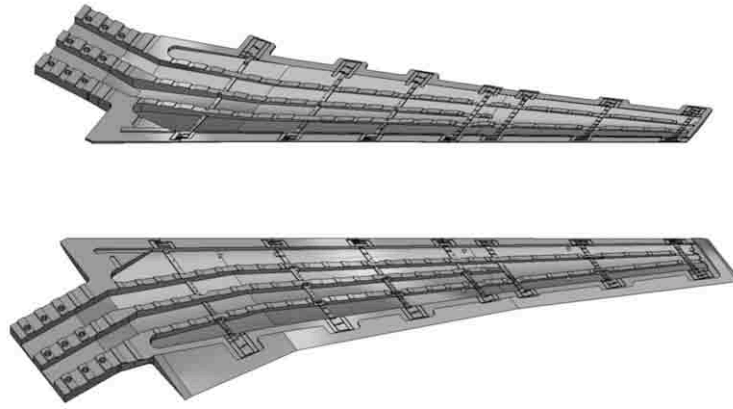
American Institute of Aeronautics and Astronautics

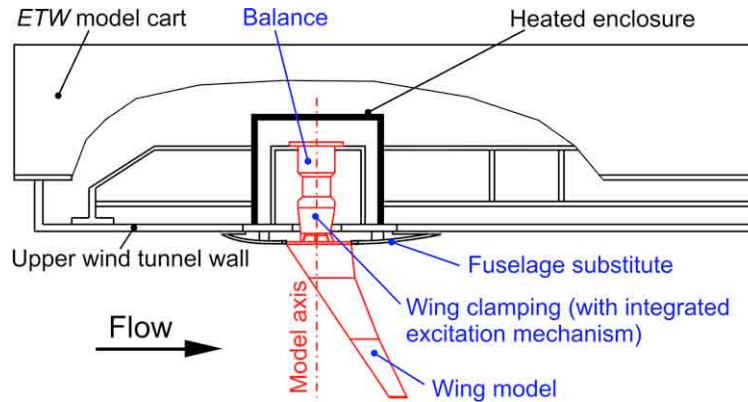**Figure 5. Inside view of the parts of the windtunnel wing.**



**Figure 6. Sketch of the placement of the total assembly in the windtunnel.**

balance in ETW had been originally designed for precise measurement in stationary testing. It is by far not stiff enough for dynamic measurements. The new balance is very stiff, the frequencies of its lowest eigenmodes are beyond $800Hz$ whereas the highest planned excitation frequency in the HIRENASD experiments was below $300Hz$.

### III.B.2. Pressure Sensors

The wing model had been equipped with 259 cryogenic miniature/ultraminiature pressure sensors (kulites) which were implemented in 7 span-wise cross sections. The relative span positions $\eta$ of these 7 cross-sections are depicted in figure 7. Because of the space needed for the sensor implementation in the interiour of the wing the sensors and pressure holes on the bottom side of the wing model are shifted about $2mm$ towards the tip relative to the pressure holes of the top side. Unfortunatelly, not all but 205 sensors were measuring correctly. On the right hand side of figure 7 the numbers of sensors which were functioning during the experiments are exemplarily presented for three measuring sections.

### III.B.3. Strain Gauges and Acceleration Sensors

The windtunnel model assembly was equipped with 28 strain gauges of which 6 were placed in the wing clamping at the excitation force transmitters and the other 22 were distributed inside the wing model as shown in figure 8. For monitoring acceleration during the tests several acceleration sensors were placed in the assembly, 11 from these accelerometers were implemented inside the model, all at the upper part of the wing model as shown in figure 9. Figure 10 shows a photograph of the full measurement implementation in the wing model before the assemblage of the two model parts.

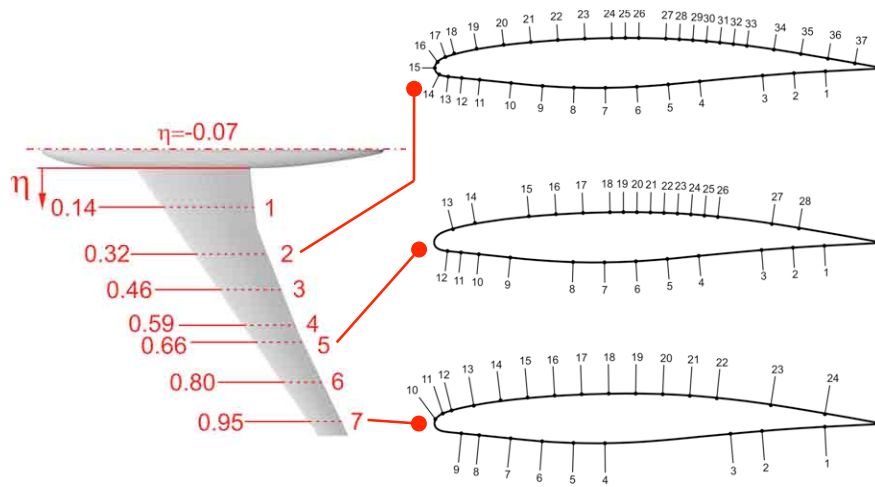American Institute of Aeronautics and Astronautics

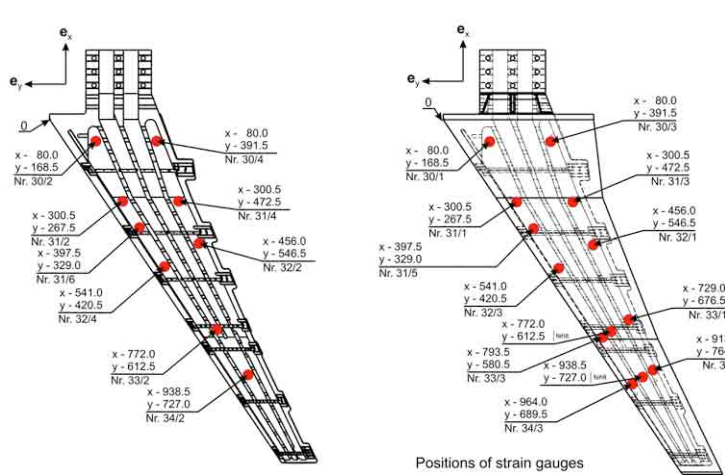Figure 7.  Model instrumentation with pressure sensors.



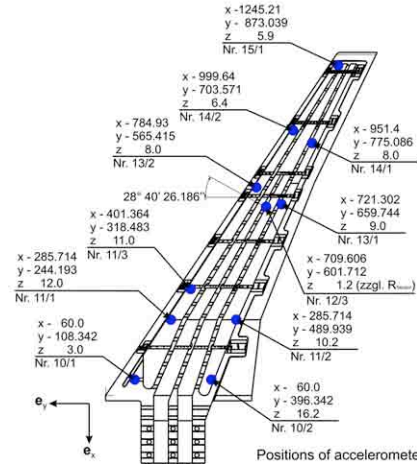Figure 8.  Positions of strain gauges inside of the wing model.



Figure 9.  Positions of accelerometers inside of the wing model.

*III.B.4.  Deformation Measurement using Stereo Pattern Tracking (SPT)*

An optical system (System picCOLOR) using ultra high speed cameras and frame grabbers was installed for displacement measurement by means of optical marker tracing. The markers were placed on the pressure side of the wing model, see left photograph of figure 3. A new high speed link for the frame transfer was established by ETW using fibre optic cables. New high power flash lights with an operating frequency up to $1kHz$ were designed in the project and installed by ETW for the model deformation system.

## IV.  Test Program and Conduction of Tests

### IV.A.  Static Tests

As mentioned in the introduction tests have been conducted for many windtunnel conditions, the main conditions were those for Mach number Ma = 0.8, for which the test envelope is presented in figure 11. The numbering corresponds to the sequence of the performed test series. During each series the values of q/E and Reynolds number are fixed. Series 1 to 4 were conducted with transition band fixed at 12% chord on the body side section and at 15% chord on the two outer sections of the suction side and continuously at 5% chord on the pressure side. Thereafter, the transition bands were removed. Originally it was planned that more tests should be made at total pressure $p_{tot} = 0.45MPa$, but during the test runs it was decided to concentrate on three lower levels, corresponding to q/E = $0.22 \cdot 10^{-6}, 0.34 \cdot 10^{-6}$ and $0.48 \cdot 10^{-6}$. With increasing values of
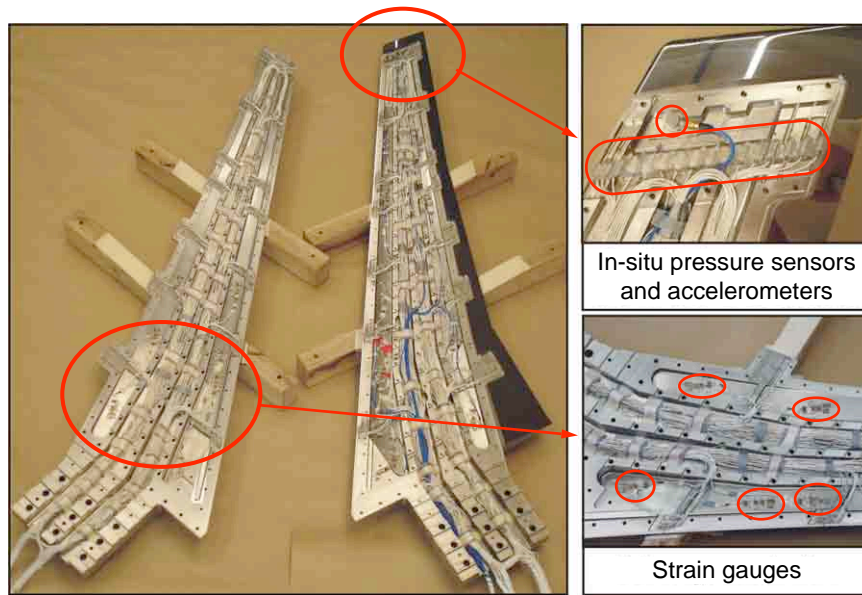
Figure 10. Model parts equipped with complete measurement implementation before assembling.

q/E the wing deformation increases and consequently the changes in the pressure distribution grow for fixed Mach and Reynolds numbers. This can be analysed looking at the results of series 6, 10 and 5 or 11. For Reynolds number effects series 2, 10, 7 or 3, 5, 8 can be studied. Similar test polars as for Ma = 0.8 were used for different Mach numbers to analyse the effect of Mach number changes.

In each series, first the static polars were measured for all Mach numbers of the series at angles of attack
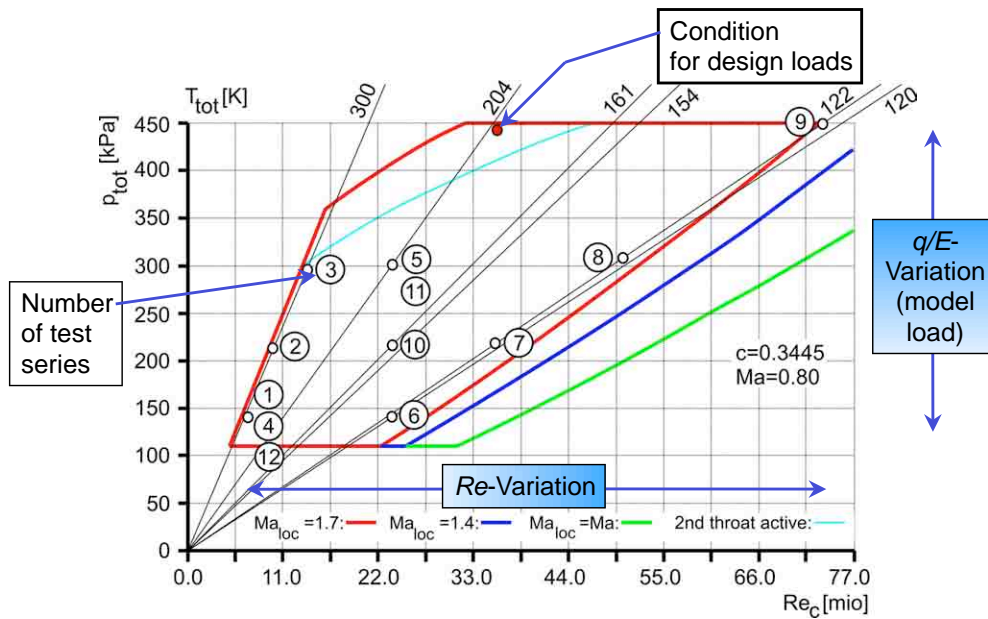


Figure 11. Windtunnel test envelope for Mach number Ma = 0.8.

from $\alpha = -2^o$ to positive angles corresponding to the load limits admitted by ETW for the model assembly, e.g. $\alpha = +4.2^o$. The angle of incidence has been changed continuously with an angular velocity of about 0.2 degrees per second. Data has been recorded with $4kHz$ in most static experiments, except the slower SPT deformation measurement, for which an exemplary result is depicted in figure 12. It contains the change of aerodynamic twist over the angle of incidence for three levels of q/E taken from the test series 1, 2, 3 (symbols) in comparison to results from numerical simulations using SOFIA taken from [11]. The

American Institute of Aeronautics and Astronautics
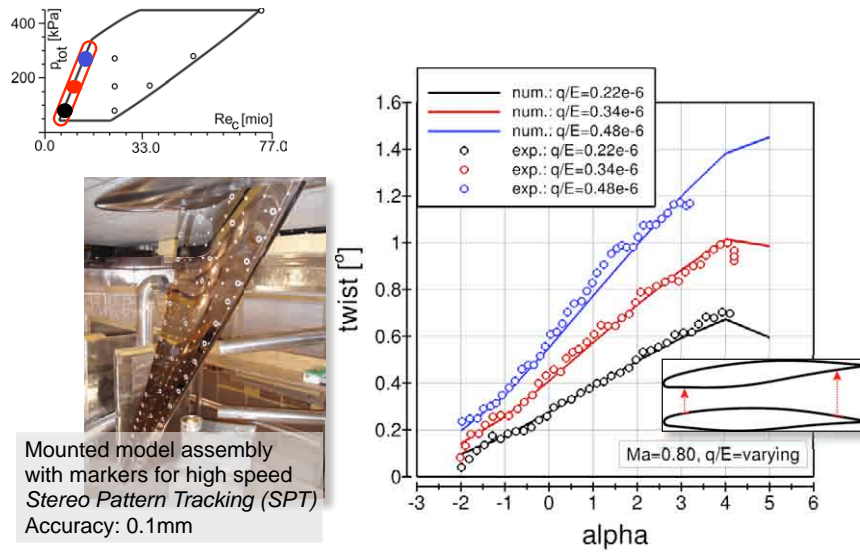
**Figure 12. Aerodynamic twist from measurements using SPT for the different levels of q/E ($= 0.22 \cdot 10^{-6}, 0.34 \cdot 10^{-6}, 0.48 \cdot 10^{-6}$) compared with results from computations using the SOFIA package.**

aerodynamic twist reached values between 0.7 and 1.2 degrees in the experiments which is mainly due to wing bending in combination with sweep. During the static polar measurements perturbations have been observed which excited the wing model to small vibrations. The frequencies of these vibrations were recorded by the acceleration sensors in the wing model, and some of these sensor signals have been evaluated online to provide values for the vibration excitation near resonance in the dynamic tests following immediately afterwards in the same measurement series.

## IV.B.  Dynamic Tests

Dynamic tests were performed for three frequencies, the first and the second mode with frequencies around $27Hz$ and $79Hz$, which are bending dominated, and the first torsion dominated mode with frequency around $265Hz$. In each series, first dynamic tests were trials without wind and tests under wind followed thereafter. Two power levels were chosen for the excitation and controlled by the voltage applied to the piezo-electric excitation stacks. For each excitation test a number of 40 blocks with 16 periods of vibration in each block was chosen, consisting of e.g. the sequence 2 blocks for noise recording, 13 blocks with 60% excitation voltage, 6 blocks without excitation, 13 blocks with 90% excitation voltage and finally 6 blocks without excitation. In each vibration period 128 data were recorded from every of the more than 300 sensor signals. The concept of 40 blocks for each vibration test has been maintained for the three tested frequencies, i.e. the test for the lowest frequency has about 10 times the duration of the tests for the torsion dominated frequency (see figure 13). More information about the dynamic qualification of the elastic wing model, including frequency and mode shape analysis, can be found in [12].

# V.  Selected Results from the Experiments in ETW

## V.A.  Static Tests

### V.A.1.  Influence of q/E Variation on Lift and Pressure Distribution

One result for Ma = 0.8 and Re = 23.5 million, where the flow is already fully turbulent almost everywhere, is depicted for varied q/E in figure 15. It can be observed that the lift decreases with increasing q/E due to the aerodynamic twist by deformation which diminishes the local angle of attack. This diminution increases in span-wise direction. The pressure distribution for one root angle of attack is presented in figure 16.
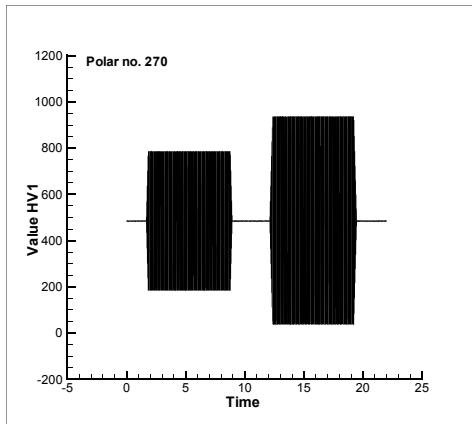
American Institute of Aeronautics and Astronautics

**Figure 13. Voltage amplitudes at piezo stack no. 1 for excitation frequency 29.1 Hz over the duration of the experiment.**
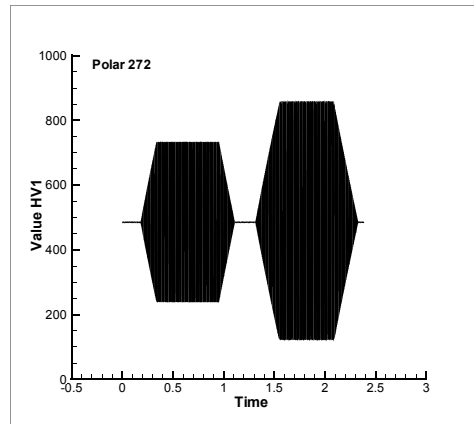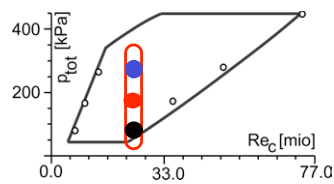


**Figure 14. Voltage amplitudes at piezo stack no. 1 for excitation frequency 268.3 Hz over the duration of the experiment.**
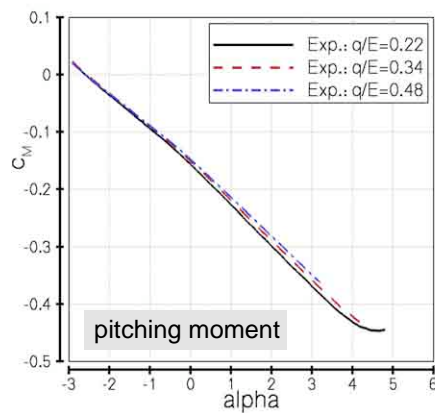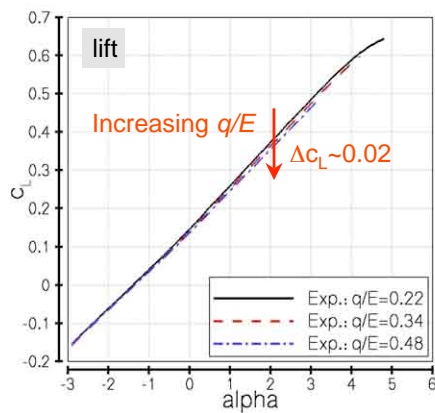


*Ma*=0.80, *Re*=23.5 mio.

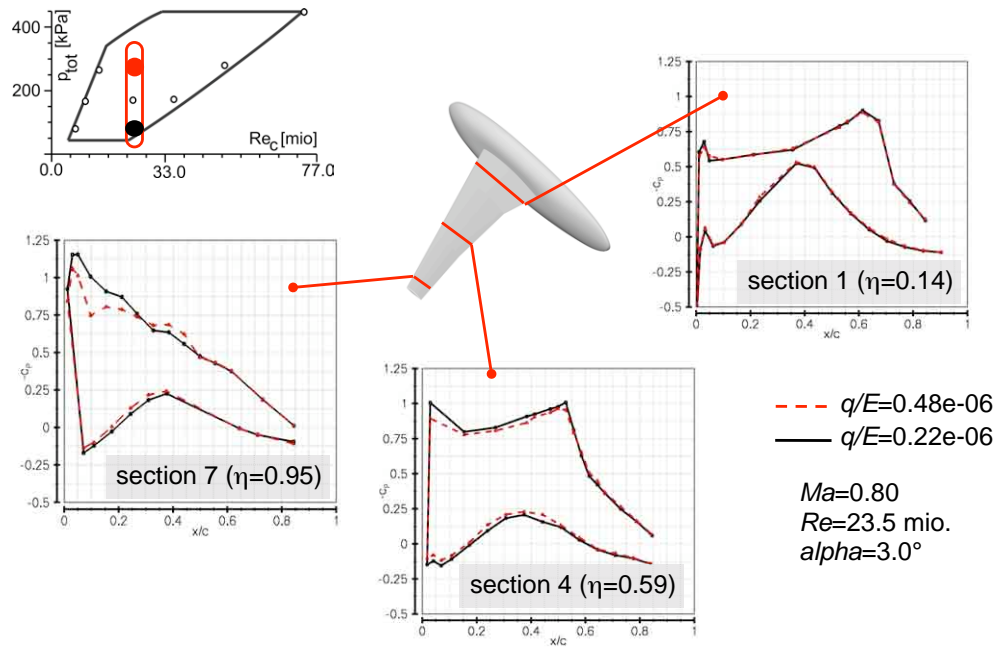**Figure 15. Influence of varying q/E on lift force and pitching moment.**

**Figure 16. Influence of varying q/E on pressure distributions in three wing sections.**
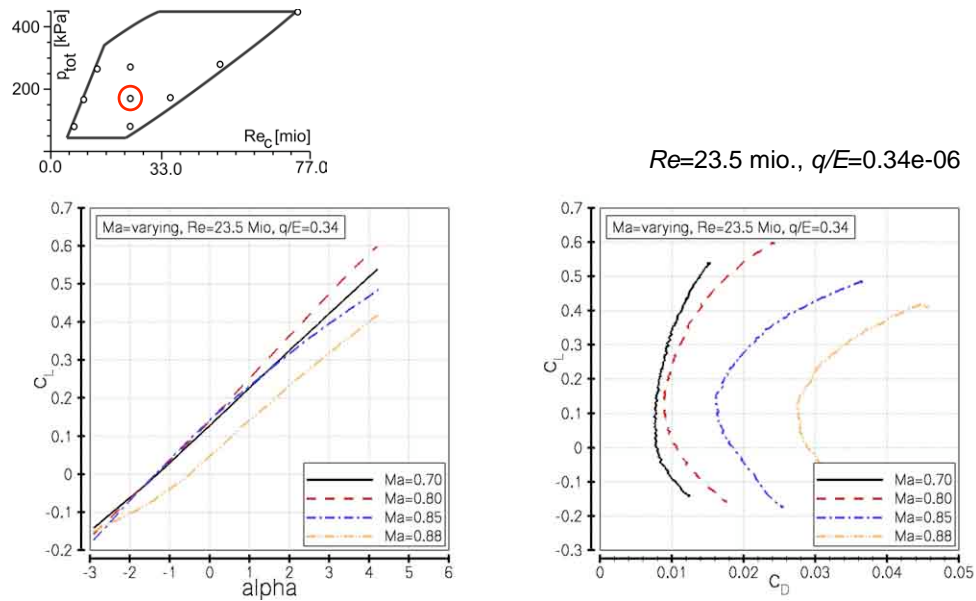


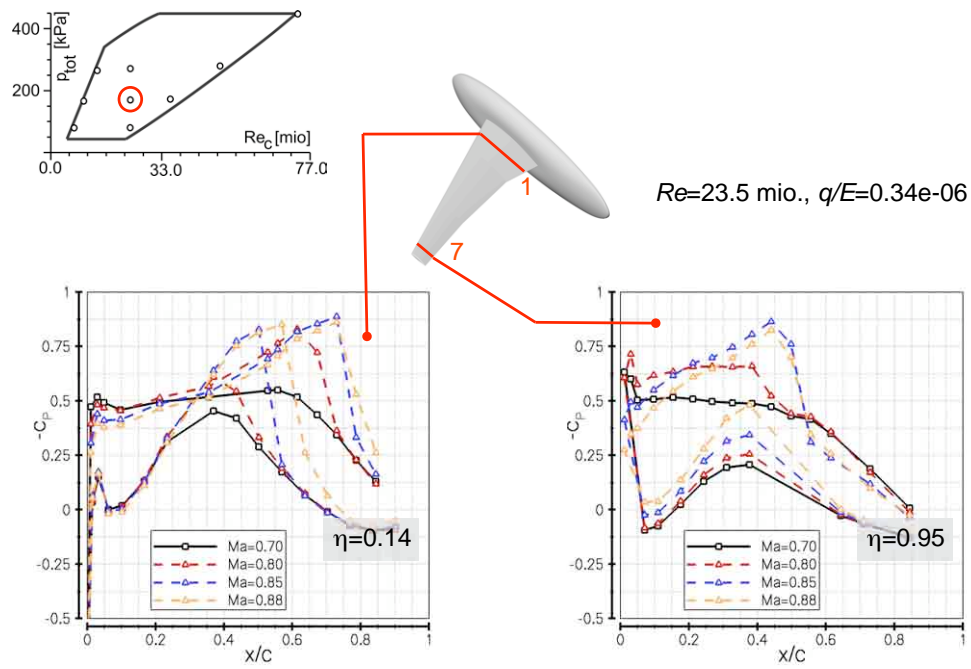**Figure 17. Influence of varying Mach number on lift and drag.**

American Institute of Aeronautics and Astronautics

**Figure 18.** Influence of varying Mach number on pressure distribution in two wing sections, $\alpha = 2^o$.
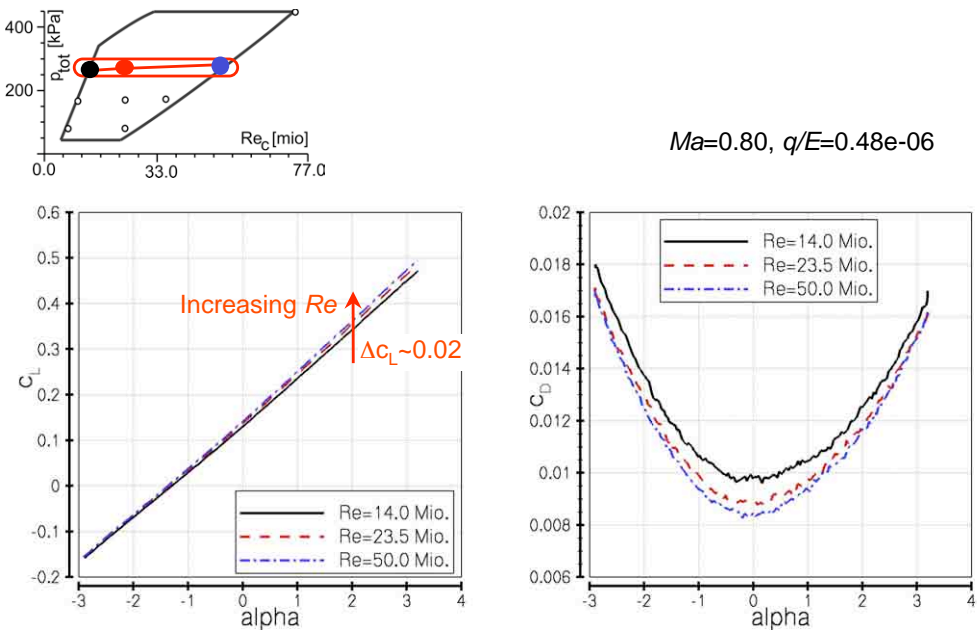


**Figure 19.** Influence of varying Reynolds number on lift and drag.
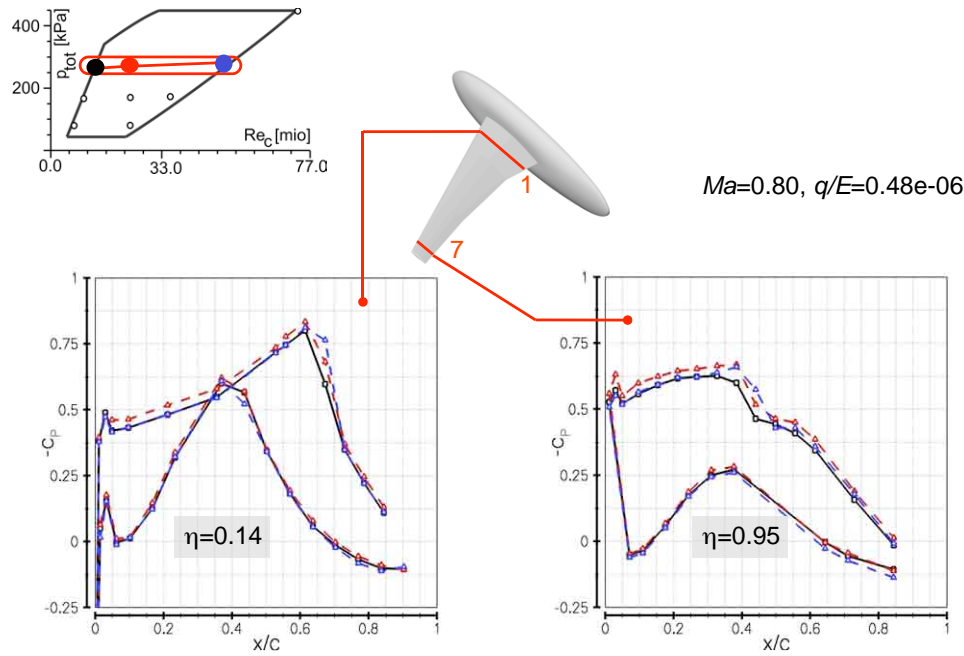
American Institute of Aeronautics and Astronautics

Figure 20. Influence of varying Reynolds number on pressure distribution in two wing sections, $\alpha = 2^o$.

### V.A.2. Influence of Mach Number Variation on Lift and Drag

Mach number varies around Ma = 0.8 for fixed $q/E = 0.34 \cdot 10^{-6}$ and Re = 23.5 million in figures 17 and 18, where lift over $\alpha$ and lift over drag polars are presented in the one and pressure distribution in two wing sections in the other figure for four Mach numbers at $\alpha = 2^o$ root angle of incidence. As can be seen lift deteroriates due to compressibility effects at Ma = 0.88. The changes of shock strength and position due to variations of the Mach number can be seen very clearly in figure 18. For Ma = 0.7 no shock is present at all.

### V.A.3. Influence of Varying Reynolds Number

Results are presented from polars of series 3, 5 and 8. Contrary to the lift decrease when increasing q/E the lift rises slightly with ascending Reynolds number and drag over $\alpha$ descends with increasing Reynolds number as is shown in figure 19. Pressure distribution in wing sections 1 and 7 are presented in figure 20 for $\alpha = 2^o$. The lift contribution of the suction side seems to be a little higher for Re = 23.5 million than for Re = 50.0 million, where in both cases the flow is fully turbulent and no transition band is present. In case of Re = 14.0 million transition bands are applied which may have some differing influence by themselves due to their dimensions.

## V.B. Dynamic Tests

Three experimental results are presented which belong to the series 5 with Re = 23.5 million and $q/E = 0.48 \cdot 10^{-6}$ at Ma = 0.8 and zero lift angle of attack which is $\alpha = -1.34^o$. The results presented in figures 21, 22 and 23 belong to the first bending dominated mode which was excited with $29.1 Hz$, the second bending dominated mode which was excited with $80.3 Hz$ and the first torsion dominated mode which was excited with $268.3 Hz$.

In all three figures the range of pressure values recorded in wing section 7 is presented in the right upper picture. The picture in the upper left corner shows the respective mode shape. The pictures at the bottom of the figures present the pressure distributions in section 7 recorded over a small interval of time interval in the 90% voltage excitation blocks which corresponds to only 4 periods in the fully excited state. The left picture shows the original data record whilst the right one presents the filtered data. Filtering was executed by means of Fourier analysis and inverse Fourier transformation using a small frequency band around the excitation frequency. The original measuring data appear very noisy. Noise is mainly due to flow disturbances from the windtunnel or from the model itself which has to be analysed deeper in the ongoing evaluation. The

American Institute of Aeronautics and Astronautics

strongest influence of noise was detected for the lowest mode frequency. Pressure perturbations in the rear part of the suction side of the wing have been analysed and were found to travel upstream from the trailing edge versus the shock which closes the supersonic range on the suction side of the wing. This phenomenon is well known e.g. from blade vortex interaction at helicopter blades when the vortex passes the trailing edge of the blade on its underside.
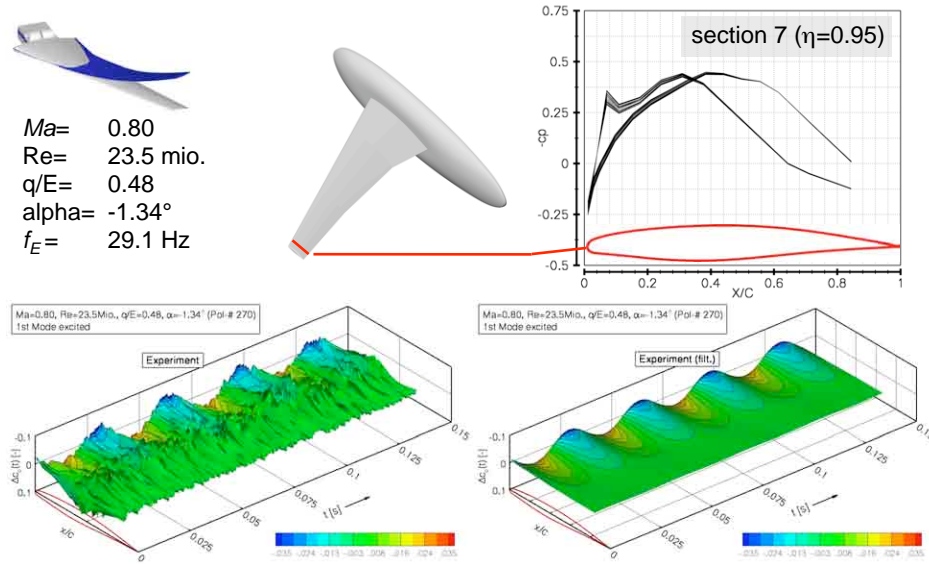


**Figure 21. Results for excitation of the first bending dominated mode near resonance for a time interval of about 4 periods in the 90% excitation blocks.**
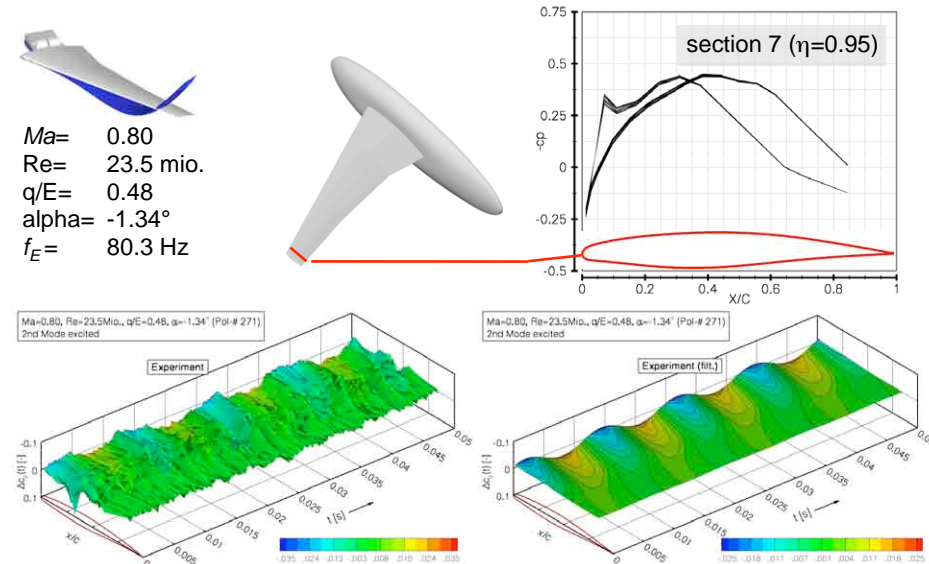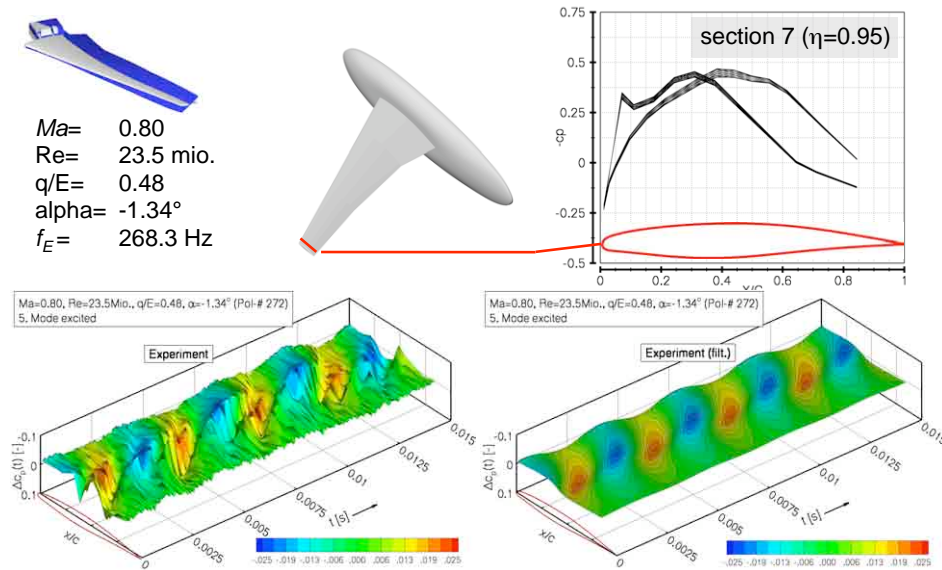


**Figure 22. Results for excitation of the second bending dominated mode near resonance for a time interval of about 4 periods in the 90% excitation blocks.**

# VI.  Conclusion

Static and dynamic aeroelastic experiments with a dynamically excited elastic wing model have been reported which were conducted in the European Transonic Windtunnel (ETW) at Reynolds numbers up to real flight conditions of large passenger aircrafts in cruise. Those conditions can be provided in ETW using cryogenic flow of nitrogen gas at high total pressure and correspondingly high dynamic pressure in transonic

American Institute of Aeronautics and Astronautics

**Figure 23.** Results for excitation of the first torsion dominated mode near resonance for a time interval of about 4 periods in the 90% excitation blocks.

flow. The aerodynamic loads on the HIRENASD model with its reference area $A_{ref} = 0.39255m^2$ exceeded two tons. Therefore, safety of model and windtunnel required a stiff construction which is difficult to excite for vibration amplitudes in the range of several percent of span. A piezoelectric mechanism was constructed to excite the whole wing by strong interior force couples in the wing clamping zone. To the knowledge of the authors it was the first time that aero-structural dynamic experiments under the described conditions have been performed. So, the experiments reported in this paper are pioneering work in some sense. Only a limited part of the obtained large amount of data has been evaluated up to now. For several reasons evaluation is not as straight forward as it might be for aeroelastic experiments in traditional windtunnels with well-known flow properties in all details and cheep and long measuring time intervals for each single experiment and a narrow band of aerodynamic loads. For the experiments presented in this paper the aerodynamic load parameter q/E varied from $0.22 \cdot 10^{-6}$ to $0.7 \cdot 10^{-6}$ and measuring time intervals had to be chosen very short because of the high expenses to provide the intended flow conditions. Evaluation is still in progress, and it will be published more about the results in the near future.

## Acknowledgments

## References

[1]Cole, S.R., Noll, T.E., Perry, B. III: Transonic Dynamics Tunnel Aeroelastic Testing in Support of Aircraft Development. Journal of Aircraft, Vol. 40, No. 5, 2003.

[2]Bartels, R.E., Edwards, J.W.: Cryogenic Tunnel Pressure Measurements on a Supercritical Airfoil for Several Shock Buffet Conditions. NASA TM-110272, 1997

[3]Ballmann J. (Ed.): Flow Modulation and Fluid-Structure Interaction at Airplane Wings. Notes On Numerical Fluid Mechanics And Multidisciplinary Design, Vol. 84, pp. 105-122, Springer, 2003

[4]Özger, E., Schell, I., Jacob, D.: On the Structure and Attenuation of an Aircraft Wake. AIAA Journal of Aircraft, Vol. 38, No. 5, pp. 878-887, 2001

[5]Moir, I.-R.M.: Measurements on a two-dimensional aerofoil with high-lift devices. AGARD-AR-303, Vol. II, 58-59, 1994

[6]Wright, M.C.N.: Half Model Testing at ETW. Technical Memorandum ETW/TM/2000028, 2000

[7]Wigley, D.A. (prep.): ETW Materials Guide Document, ETW/D/95005, 1996

[8]Ballmann, J., Dafnis, A.: Challenges of Nonsmooth Mechanics in Aero-Structural Dynamics, in C. C. Baniotopoulos (ed.), Nonsmooth/Nonconvex Mechanics with Applications in Engineering, II. NNMAE 2006, Proc. Int. Conf. Tessaloniki, 06.-08. July 2006, pp. 307-314

[9]Ballmann, J., Dafnis, A., Brakhage, K.-H., Braun, C., Kämpchen, M., Korsch, H., Reimerdes, H.-G., Olivier, H.: The HIRENASD Elastic Wing Model and Aeroelastic Test Program in the European Transonic Windtunnel (ETW). DGLR Annual Congress 2005, Paper DGLR-2005-064

[10]Braun, C., Boucke, A., Ballmann, J.: Numerical Prediction of Wing Deformation of a High Speed Transport Aircraft Type Wind Tunnel Model by Direct Aeroelastic Simulation. International Forum on Aeroelasticity and Structural Dynamics (IFASD) 2005, Munich, Germany, paper IF 147

[11]Reimer, L., Braun, C., Chen, B.H., Ballmann, J.: Computational Aeroelastic Design and Analysis of the HIRENASD Wind Tunnel Wing Model and Tests. International Forum on Aeroelasticity and Structural Dynamics (IFASD) 2007, Stockholm, Sweden, paper IF 071

[12]Dafnis, A., Korsch, H., Buxel, C., Reimerdes, H.-G.: Dynamic Response of the HIRENASD Elastic Wing Model under Wind-off and Wind-on Conditions. International Forum on Aeroelasticity and Structural Dynamics (IFASD) 2007, Stockholm, Sweden, paper IF 073